Report

Recapitulation of Developing Artery Muscularization in Pulmonary Hypertension

Abdul Q. Sheikh,[1,2] Janet K. Lighthouse,[1,2] and Daniel M. Greif[1,*]
[1]Yale Cardiovascular Research Center, Section of Cardiovascular Medicine, Department of Internal Medicine, Yale University School of Medicine, 300 George Street, Room 773J, New Haven, CT 06511, USA
[2]These authors contributed equally to this work
*Correspondence: daniel.greif@yale.edu

SUMMARY

Excess smooth muscle accumulation is a key component of many vascular disorders, including atherosclerosis, restenosis, and pulmonary artery hypertension, but the underlying cell biological processes are not well defined. In pulmonary artery hypertension, reduced pulmonary artery compliance is a strong independent predictor of mortality, and pathological distal arteriole muscularization contributes to this reduced compliance. We recently demonstrated that embryonic pulmonary artery wall morphogenesis consists of discrete developmentally regulated steps. In contrast, poor understanding of distal arteriole muscularization in pulmonary artery hypertension severely limits existing therapies that aim to dilate the pulmonary vasculature but have modest clinical benefit and do not prevent hypermuscularization. Here, we show that most pathological distal arteriole smooth muscle cells, but not alveolar myofibroblasts, derive from pre-existing smooth muscle. Furthermore, the program of distal arteriole muscularization encompasses smooth muscle cell dedifferentiation, distal migration, proliferation, and then redifferentiation, thereby recapitulating many facets of arterial wall development.

INTRODUCTION

Novel efficacious treatments for pulmonary artery hypertension (PAH) are desperately needed, given that this disease is highly morbid and lethal; indeed, ~45% of patients die within three years of initial diagnosis (Humbert et al., 2010). The histopathological findings of PAH include an increased smooth muscle cell (SMC) burden with distal extension of SMCs to normally nomuscularized pulmonary arterioles (Farber and Loscalzo, 2004). PAH results from increased resistance to flow through the pulmonary vasculature, and decreased compliance of muscularized distal arterioles is an important contributor (Rabino-

vitch, 2008). Furthermore, in PAH, reduced compliance of the pulmonary arterial vasculature is a strong independent predictor of mortality (Mahapatra et al., 2006). Existing medical therapies for PAH primarily lower pulmonary artery (PA) blood pressure through vasodilation but have modest clinical efficacy and limited ameliorative effects on SMC differentiation, migration or recruitment.

This void in therapeutic options for PAH is striking but perhaps not surprising, because our understanding of the molecular and cellular processes underlying arteriole muscularization is limited. Many signaling pathways contribute to PAH pathology (Kim et al., 2013; Rabinovitch, 2008), and although a number of cellular sources of the pathological distal arteriole SMCs have been implicated (Morrell et al., 2009; Stenmark et al., 2006), the origin of these SMCs remains to be defined. In addition, increased alpha smooth muscle actin (SMA)+ alveolar myofibroblasts have been observed in human pulmonary hypertension (PH) (Kapanci et al., 1990), but their pathogenesis has not been analyzed. We recently demonstrated that construction of the embryonic PA wall is composed of discrete developmentally regulated steps involving progenitor recruitment, migration, differentiation, and proliferation (Greif et al., 2012). Herein, through meticulous analysis of three pulmonary arteriole beds and surrounding alveoli, we now show that in hypoxia-induced PH, the distal arteriole SMCs, but not alveolar myofibroblasts, derive from pre-existing SMC marker+ cells. Furthermore, this distal arteriole muscularization encompasses a tightly regulated pathological program in which SMCs undergo dedifferentiation, distal migration, proliferation, and then redifferentiation, thereby recapitulating many aspects of the developmental program.

RESULTS

Specific Nonmuscularized Distal Arterioles Become Muscularized with Hypoxia

Currently, the extent of pulmonary vascular remodeling in PH is assessed by crudely grading the muscular coverage of individual small arterioles on random lung sections. Recently, we uncovered key insights by meticulously analyzing the construction of the wall of a small region of the left PA during normal embryogenesis (Greif et al., 2012), and herein, we have developed a similar reductionist approach to examine pulmonary arteriole
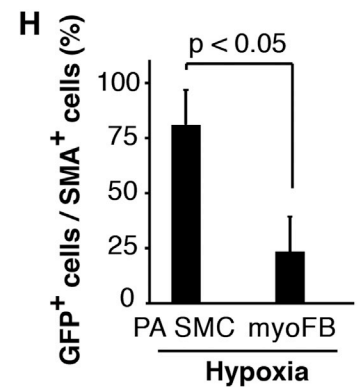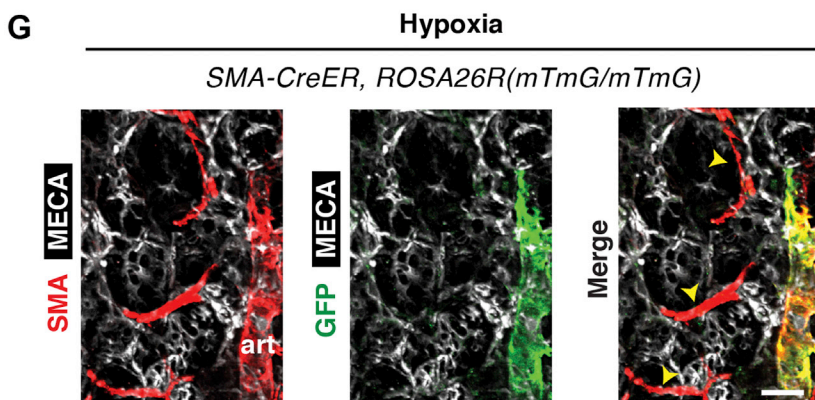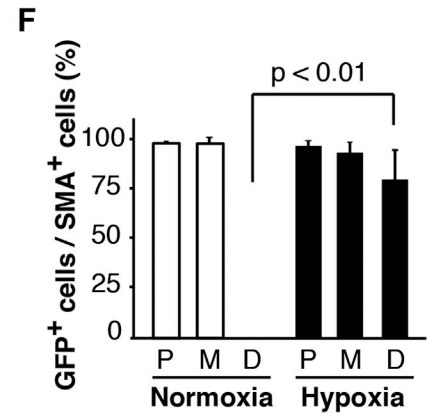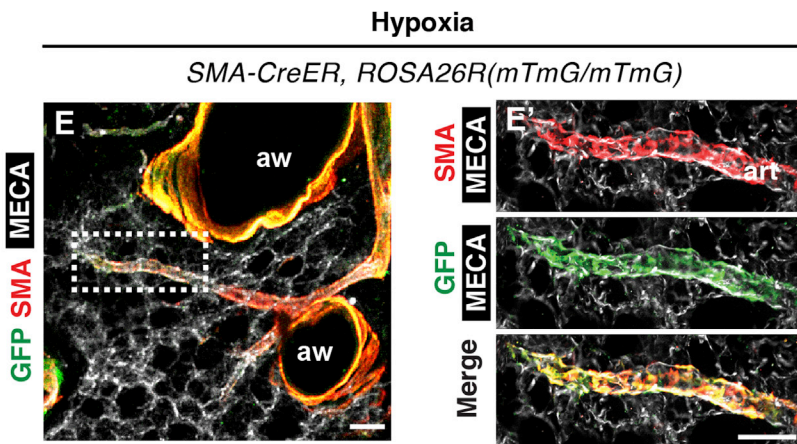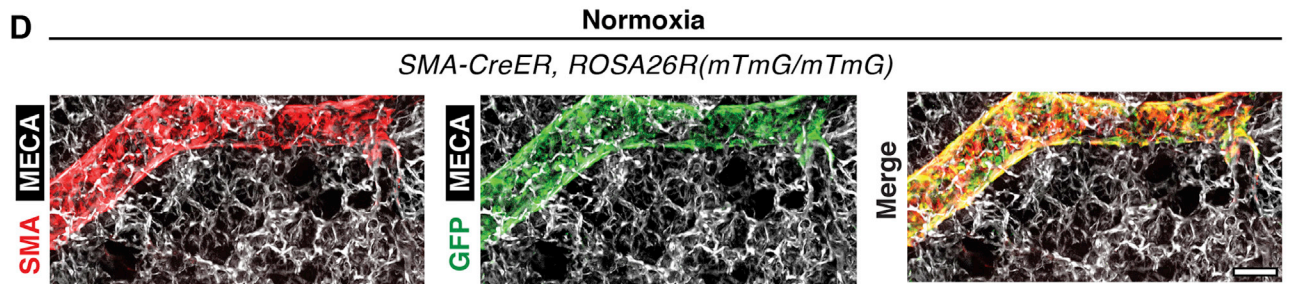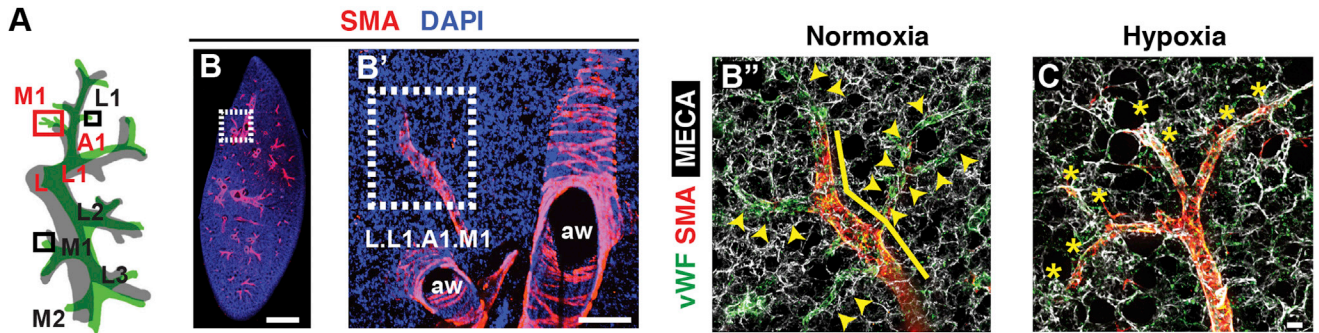
(legend on next page)

muscularization during PH onset in the adult mouse. This approach is facilitated by the stereotyped and similar pulmonary arterial and airway branching patterns, allowing for reproducible identification of specific arteriole beds (Figures S1A–S1C). We focus on three vascular beds located in the cranial and medial aspects of the adult left lung (Figures 1A, 1B, 1B′, and 1B″) and categorize the arteriole segments in each of these vascular beds (by both position in the vascular tree and lumen diameter) as proximal (>75 μm distal), middle (25–75 μm), or distal (<25 μm). Proximal and middle arterioles are coated by SMCs, whereas distal arterioles are not muscularized and extend from the middle arteriole to the capillary bed. Thus, under normal conditions, the middle-distal (M-D) arteriole border, a fixed anatomical border, coincides with the transition from muscularized to unmuscularized arteriole.

Hypoxia is a well-established independent cause of human PH and also exacerbates PH due to other etiologies, such as PAH and parenchymal lung disease (Stenmark et al., 2006). Mice exposed to hypoxia (FiO$_2$ 10%) for 3 weeks develop PH (Figure S1D) (Stenmark et al., 2006), and we noted significant right ventricle (RV) hypertrophy by 2 weeks and increasing hypertrophy over the subsequent week (Figure S1E). Importantly, with chronic hypoxia treatment, unmuscularized distal arterioles in the aforementioned vascular beds become muscularized with SMA$^+$ cells (Figure 1C). Thus, in contrast to the fixed M-D border, the muscular-unmuscular transition zone is dynamic, moving distally with hypoxia. This distal extension of SMC coverage to normally nonmuscularized pulmonary arterioles is a hallmark of human PH (Shimoda and Laurie, 2013).

Distal Pulmonary Arteriole SMCs Derive from Pre-existing SMCs

To determine whether pre-existing SMCs give rise to distal pulmonary arteriole SMCs during PH, we carried out lineage tracing with the CreER-loxP system. Tamoxifen treatment of normoxic mice carrying *SMA-CreER^{T2}* (Wendling et al., 2009)

and the Cre reporter *ROSA26R$^{(mTmG/mTmG)}$* (Muzumdar et al., 2007) induces marking of SMCs (Figures 1D and S2), and after the labeling phase (i.e., 5 days of tamoxifen [1 mg/day] and 5 days of rest), ~95% of PA SMCs express the GFP lineage tag (Figure 1F, normoxia). We then analyzed the expression of GFP in pulmonary arterioles of the aforementioned vascular beds (see Figure 1A) of *SMA-CreER, ROSA26R$^{(mTmG/mTmG)}$* mice following tamoxifen labeling, rest, and then 3 weeks of hypoxia. Interestingly, >80% of the distal pulmonary arteriole SMCs were GFP$^+$ (Figures 1E, 1E′, and 1F), indicating that pre-existing SMCs are the major source of hypoxia-induced distal arteriole smooth muscle. These studies fate map SMCs in PH and, along with our prior developmental studies (Greif et al., 2012), indicate that SMC migration along the axial direction of uncoated endothelial cell (EC) tubes is common to both the developmental and pathological programs of arterial muscularization.

Hypoxia-Induced Myofibroblasts Primarily Derive from SMA$^-$ Cells

Alveolar myofibroblasts increase in quantity during the first 2 postnatal weeks and are key players in alveolar septal formation during alveologenesis (Choi, 2010; McGowan and McCoy, 2011). Herein, we observed that the number of elongated alveolar SMA$^+$ myofibroblasts decreases by postnatal week 4 as compared to week 2, and this diminution continues until they are essentially absent in adulthood (Figures S3A and S3C). Alveolar myofibroblasts have been shown to accumulate in human PH (Kapanci et al., 1990) and increase in mice after exposure to hypoxia for 6 weeks (Chen et al., 2006). Our studies indicate that the number of myofibroblasts increases significantly within 7 days of hypoxia and continues to do so over the next 2 weeks (Figures S3B and S3C). We then utilized lineage analysis with *SMA-CreER^{T2}, ROSA26R$^{(mTmG/mTmG)}$* mice induced with tamoxifen and determined that in contrast to distal pulmonary arteriole SMCs, >75% of the alveolar myofibroblasts induced by hypoxia

Figure 1. Muscularization of Specific Distal Arterioles with Hypoxia

(A) Schematic of proximal PA (green) and airway (gray) branches of left lung (ventral view). The three boxes indicate regions where we have reproducibly identified unmuscularized distal arteriole beds that become muscularized with hypoxia. The red box indicates the arteriole bed shown in (B′), (B″), and (C). This arteriole bed is in proximity to airway branch L.L1.A1.M1 (i.e., left bronchus-first lateral secondary branch-first anterior branch-first medial branch) (Metzger et al., 2008). L, left main bronchus; L1, L2, L3, lateral branches; M1, M2, medial branches; A1, anterior branch.

(B and C) Left lungs stained for SMA (SMC marker, red), von Willebrand factor (vWF; expressed by ECs of larger vessels, green), MECA-32 (pan-EC marker, white), and nuclei (DAPI, blue). The lungs shown in (B) and (C) are harvested from adult mice after exposure to normoxia or hypoxia (FiO$_2$ 10%) for 3 weeks, respectively. The boxed region of the vibratome coronal section in (B) is shown at higher power in (B′). In (B′), muscularized airways are indicated by "aw," and the arteriole bed of interest is boxed and shown at higher power in (B″). The line and arrowheads in (B″) indicate the muscularized middle and unmuscularized distal arterioles, respectively. In (C), the distal arterioles are coated by SMA$^+$ cells up to the transition to capillaries as shown by the asterisk.

(D and E) Left lungs of adult *SMA-CreER, ROSA26R$^{(mTmG/mTmG)}$* mice induced with tamoxifen, rested for 5 days, and then either confocal imaged (D) or exposed to hypoxia for 3 weeks prior to imaging (E). Lungs were stained for SMA (red), GFP (Cre reporter, green), and MECA-32 (white). A muscularized middle arteriole and adjacent alveoli in proximity to airway L.L1.A1.L1 are shown in (D). The boxed region in (E) (shown at higher power in E′) contains a distal arteriole in proximity to the L.M1 airway branch (see A, lower black box) that we previously identified becomes muscularized with hypoxia. Note that hypoxia-induced SMCs of the distal arteriole (art) are marked with the lineage tag (GFP).

(F) Quantification of the percent of arteriole SMA$^+$ cells that are GFP$^+$, stratified by arteriole location/diameter as proximal (P; >75 μm), middle (M; 25–75 μm), or distal (D; <25 μm). The number of each pulmonary arteriole type analyzed and SMA$^+$ cells scored were: normoxia (P: 2 arterioles, 151 cells; M: 3, 181; D: 3, 0) and hypoxia (P: 5, 207; M: 8, 348; D: 9, 115).

(G) Confocal image of alveoli adjacent to distal muscularized arteriole (art; L.L1.A.L1) from a *SMA-CreER, ROSA26R$^{(mTmG/mTmG)}$* mouse both treated with tamoxifen and hypoxia and stained as in (E). Note that arteriole SMCs, but not alveolar SMA$^+$ cells (indicated by arrowhead), are marked by the GFP lineage tag.

(H) Quantification of the percent of alveolar myofibroblasts (myoFBs) that express GFP with hypoxia and compared to this percent for distal arteriole SMCs as shown in (F). The number of SMA$^+$ cells scored in the distal arterioles and alveoli were 115 (PA SMC) and 265 (myoFB), respectively.

Error bars in (F) and (H) indicate SD. Scale bars represent 1 mm (B), 100 μm (B′), and 25 μm (C, D, E, E′, and G). See also Figures S1–S3.
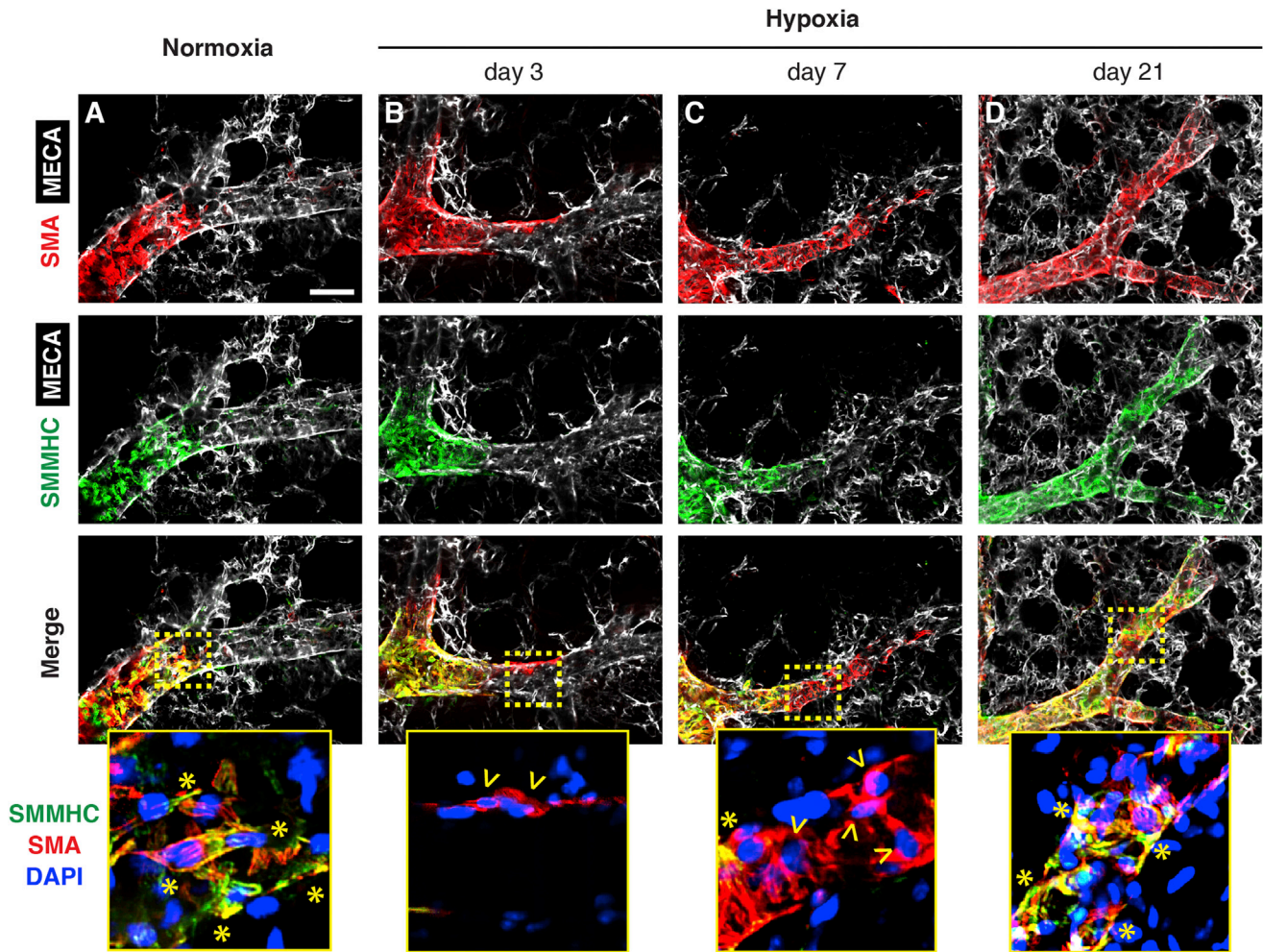
Figure 2. Dynamic and Distinct Expression of SMA and SMMHC during Hypoxia-Induced Distal Pulmonary Arteriole Muscularization

(A–D) Adult mice were exposed to normoxia or to hypoxia for 3, 7, and 21 days as indicated, and then left lungs were stained for SMA (red), SMMHC (green), MECA-32 (white), and nuclei (DAPI, blue). Representative confocal images of arteriole beds located in proximity to L.L1.A1 airway branches. The boxed regions in the merged images are shown as close-ups below with asterisks and open arrowheads representing SMA⁺SMMHC⁺ and SMA⁺ cells, respectively. Note the transitory downregulation of SMMHC in SMA⁺ cells in the distal arteriole at 3 and 7 days of hypoxia. Scale bar, 25 μm. See also Figures S3 and S4.

are GFP⁻ and thus arise from SMA⁻ cells that were present prior to hypoxia treatment (Figures 1G and 1H). Prior studies have not utilized genetic tracing to evaluate the cellular origin of hypoxia-induced alveolar myofibroblasts.

Initial Distal Arteriole Muscularization Involves SMC Dedifferentiation

We next examined a timeline of cellular and molecular events during SMC invasion of distal arterioles with PH onset. We first evaluated the normoxia and initial week of hypoxia time periods, focusing on the expression patterns of SMA, the differentiated SMC marker smooth muscle myosin heavy chain (SMMHC), and the undifferentiated mesenchymal marker platelet-derived growth factor receptor-β (PDGFR-β; Figures 2, 3, and S4). Under normoxic conditions, SMMHC and SMA are expressed in the same pulmonary arteriole cells (Figures 2A and S4A), whereas arteriole PDGFR-β expression is limited to a few SMC marker⁺

cells located at or near the muscular-unmuscular transition zone (i.e., the normoxic M-D border; Figures 3A, 3A′, and S4A). By day 3 of hypoxia, a few SMA⁺SMMHC⁻ cells are located just distal to the M-D border (Figure 2B), and many of these cells express PDGFR-β (Figures 3B and S4B). Given the fate-mapping findings (Figures 1E and 1F), we suggest these cells derive from pre-existing arteriole SMCs and upon hypoxia exposure dedifferentiate (i.e., decrease SMMHC expression and increase PDGFR-β expression) and migrate across the M-D border. By day 7 of hypoxia, the process of arteriole muscularization with SMA⁺SMMHC⁻ cells has continued distally down the arteriole (Figures 2C and S4C), and these SMA⁺ cells also express PDGFR-β (Figures 3C and S4C). Meanwhile, the distal arteriole SMA⁺ cells located in proximity to the M-D border have begun to express SMMHC (Figure 2C). SMC dedifferentiation is not observed in normal PA wall morphogenesis (Greif et al., 2012); however, both the developmental and disease
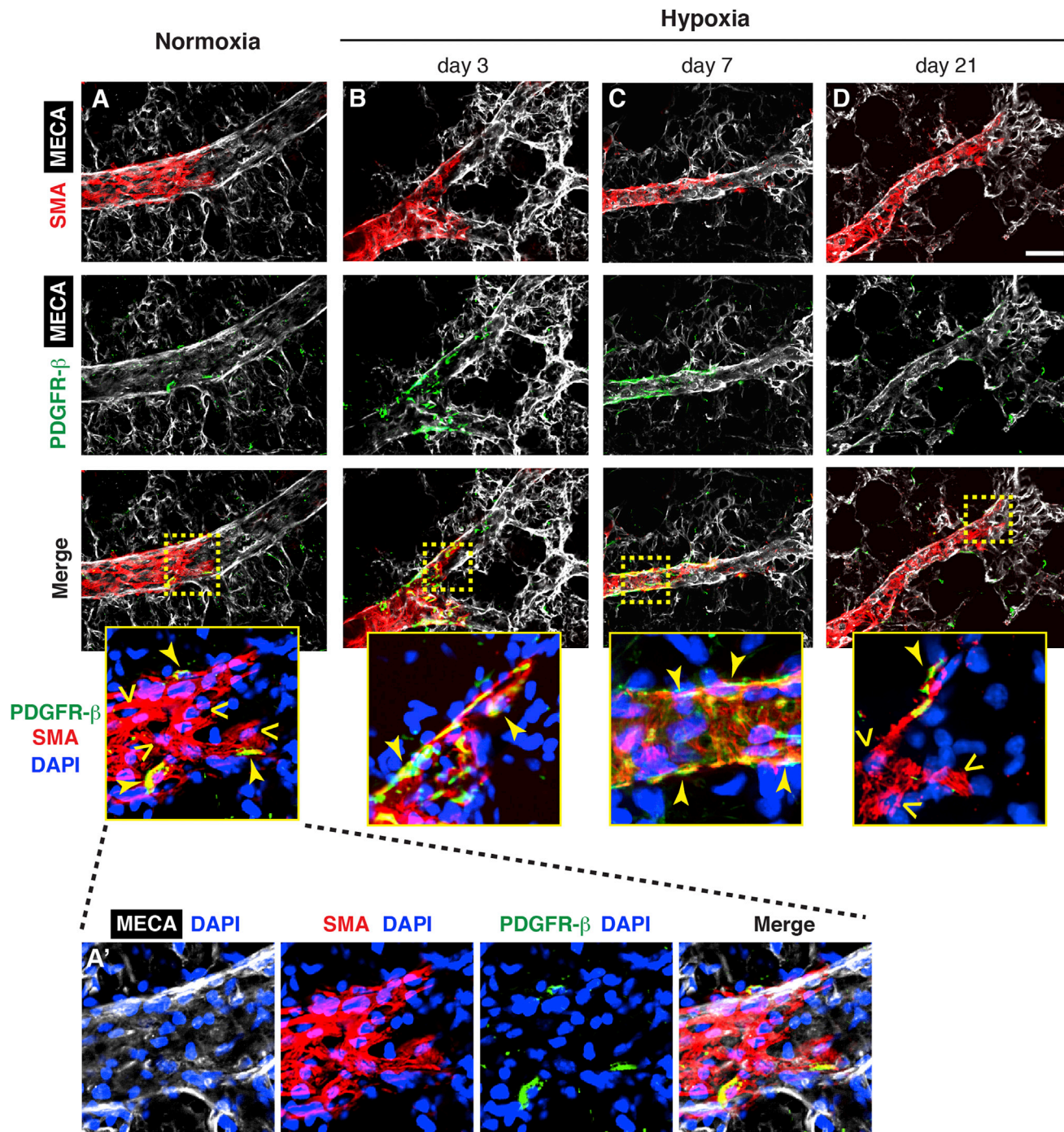
Figure 3. PDGFR-β Expression Pattern during Hypoxia Indicates Distal Arteriole SMC Dedifferentiation and Redifferentiation

(A–D) Distal arterioles in the aforementioned arteriole beds (see Figure 1A) at the indicated time points of hypoxia stained for SMA (red), PDGFR-β (green), MECA-32 (white), and nuclei (DAPI, blue). The boxed regions in the merged images are shown as close-ups below with open and closed arrowheads representing SMA[+] and SMA[+]PDGFR-β^{+} cells, respectively. Note the transitory broad expression of PDGFR-β in distal arteriole SMA^{+} cells at days 3 and 7 of hypoxia. The close-up in (A) is shown below (in A′) in individual panels with DAPI and specific channels as well as a merge of all channels. Scale bar, 25 μm. See also Figure S4.

muscularization programs are characterized by SMA^{+} cells that have transitory expression of PDGFR-β and robustly both migrate and, as described below, proliferate (see Figures 4A and 4B).

Differentiation of Hypoxia-Induced Arteriole Smooth Muscle and Alveolar Myofibroblasts

During the second week of hypoxia, SMA^{+} cells continue to migrate distally along the pulmonary arteriole and, interestingly,

Figure 4. Hypoxia-Induced Distal Arteriole SMC Proliferation and Schematic of Key Events during Distal Muscularization

(A) Distal arterioles in proximity to L.L1.A1 airway branches at normoxia or indicated days of hypoxia stained for SMA (red), BrdU (green), CD31 (EC marker, white), and nuclei (DAPI, blue).

by day 14, begin to upregulate SMMHC expression (Figures S4D and S4F). Concomitantly, PDGFR-β expression is decreasing in SMA⁺ cells with SMA⁺PDGFR-β⁺ cells detectable in a discontinuous fashion in the distal arteriole (Figures S4D and S4G). The differentiation process continues until day 21 of hypoxia, when SMA⁺SMMHC⁺ cells coat essentially the entire distal arteriole up to the lung capillaries (Figures 2D and S4E). At this time point, PDGFR-β is not detectable throughout the pulmonary arteriole, except for a few SMA⁺SMMHC⁺PDGFR-β⁺ cells located in proximity to the new muscular-unmuscular transition zone (Figures 3D and S4E); interestingly, this pattern is similar to what was noted in the normoxic condition (see Figures 3A and S4A). Furthermore, this phase of hypoxia-induced distal arteriole smooth muscle maturation recapitulates the program of normal embryonic PA wall differentiation in which smooth muscle layers undergo developmentally regulated and coordinated SMC marker expression and PDGFR-β downregulation (Greif et al., 2012).

In addition to hypermuscularization of the pulmonary vasculature, the number of alveolar SMA⁺ myofibroblasts also progressively increases with hypoxia treatment (see Figures S3B and S3C). These alveolar SMA⁺ cells markedly upregulate SMMHC, with ∼85% of alveolar SMA⁺ myofibroblasts also expressing SMMHC by day 21 of hypoxia (Figures S3D and S3E). In contrast, PDGFR-β expression was not detected in these cells at any stage (data not shown).

Distal Arteriole Smooth Muscle Proliferation Peaks at 1 Week of Hypoxia

We then investigated alveolar myofibroblast and pulmonary arteriole cell proliferation during hypoxia by assessing bromodeoxyuridine (BrdU) incorporation 4 hours after a single intraperitoneal injection (Figures 4A–4C and S1F). A very low percentage of alveolar myofibroblasts were proliferative at each time point evaluated (i.e., normoxia and hypoxia days 3, 7, 14, and 21); combining all time points, only 4 of the 394 myofibroblasts scored were BrdU⁺ (Figure 4C; data not shown). In contrast, EC proliferation is significantly increased in middle and distal pulmonary arterioles by day 21 of hypoxia (Figure S1F). Similar to the myofibroblast results, very rare BrdU⁺ SMCs in the proximal or middle arteriole were detected under normoxic and all hypoxic conditions (Figure 4B). Although SMCs begin to migrate distally by day 3 of hypoxia, only ∼5% of distal arteriole SMCs are BrdU⁺ (Figures 4A and 4B), suggesting that initial muscularization is driven primarily by migration and not proliferation. In contrast, by day 7, there is marked upregulation in distal proliferation with, remarkably, ∼65% of distal arteriole SMCs staining for BrdU. Subsequently, this proliferation decreases, and by 21 days of hypoxia, the proliferation rate returns to that of normoxia. These pathological findings are comparable to our prior developmental results that at the midpoint of normal embryonic PA morphogenesis, SMA⁺ wall cells maintain a significant proliferative index (Greif et al., 2012).

DISCUSSION

A critical component of the massive burden of cardiovascular disease on human health is the excessive and ectopic accumulation of SMCs that plagues numerous arterial diseases, including atherosclerosis, restenosis after balloon angioplasty, and PAH. Unfortunately, little is known regarding the in vivo molecular and cellular processes underlying these pathologies, and this lack of knowledge severely limits therapeutic options (Gomez and Owens, 2012; Seidelmann et al., 2013). Distal pulmonary arteriole muscularization is a critical component of PAH pathophysiology, and herein, we utilize fate mapping and develop an approach for generating a timeline of key molecular and cellular events during hypoxia-induced muscularization of specific distal arteriole beds.

Our fate-mapping results indicate that the vast majority of hypoxia-induced distal arteriole SMCs derive from pre-existing smooth muscle. Previous studies have also proposed other potential cellular sources for the excess SMCs in PH, including fibroblasts, pericytes, ECs, and hematopoietic cells (Hayashida et al., 2005; Morrell et al., 2009; Qiao et al., 2013; Spees et al., 2008; Stenmark et al., 2006). The only prior lineage analysis in PH was recently reported and used constitutive Cre's driven by the promoters of vascular endothelial-cadherin or Tie2 in the context of a new murine PH model of surgical pneumonectomy followed by monocrotaline injection (Qiao et al., 2013). The authors conclude that in this PH model, a minority of PA SMCs derive from ECs; however, the contribution of such transdifferentiation to distal pulmonary arteriole muscularization is not clear given anatomical considerations, non-EC recombination, and potential PA EC transdifferentiation to SMCs during embryogenesis (Arciniegas et al., 2000; Jiao et al., 2006; Morimoto et al., 2010; Qiao et al., 2013). In addition, bone marrow transplant studies suggest that bone marrow-derived cells contribute to a

---

(B) Quantification of proliferating SMCs in proximal (P), middle (M), and distal (D) arterioles in the regions noted in (A) at the indicated time points. At least eight arterioles were analyzed for each normoxia or hypoxia condition, and the number of SMA⁺ cells scored for each condition by arteriole type was P (each condition, 180–205 SMA⁺ cells), M (each condition, 130–190), or D (normoxia, 0; hypoxia 3 days, 20; 7 days, 39; 14 days, 88; 21 days, 130). Note the robust increase in distal arteriole SMC proliferation at days 7 and 14. ε versus normoxia D, p < 0.005; # versus hypoxia P and M, p < 0.005. Error bars indicate SD.

(C) Alveoli and distal arteriole (art) in proximity to L.L1.A1.L1 airway branch at hypoxia day 7 stained as in (A). Asterisks indicate BrdU⁺SMA⁺ distal arteriole cells whereas the alveolar myofibroblasts (arrowheads) do not stain for BrdU.

(D) Summary of molecular and cellular events during hypoxia-induced distal pulmonary arteriole muscularization. Under normoxic conditions, M (and P) arteriole SMCs are SMA⁺SMMHC⁺ (gray), and the D arteriole is not muscularized. Interestingly, a few rare SMA⁺SMMHC⁺PDGFR-β⁺ cells (yellow) are located just proximal to the M-D border (dashed vertical line). By day 3 of hypoxia, the pre-existing SMCs have started to migrate distally across the M-D border and dedifferentiate as indicated by the expression of PDGFR-β and downregulation of SMMHC (pink). These cells are proliferative (dividing cell) by day 7 and continue to migrate distally. At day 14, proliferation continues and distal arteriole SMA⁺ cells start to redifferentiate as indicated by the expression of SMMHC and downregulation of PDGFR-β. By day 21 of hypoxia, essentially the entire distal pulmonary arteriole is coated with nonproliferative, differentiated SMCs (gray) and, similar to the normoxic condition, a few SMA⁺SMMHC⁺PDGFR-β⁺ are located adjacent to the new muscular-unmuscular transition zone.

Scale bars, 25 μm. See also Figure S1.

number of lung cell types in PH, including SMA^{+} vascular cells (Hayashida et al., 2005; Spees et al., 2008), which is potentially consistent with our findings as SMA is expressed in select bone marrow-derived cells (Peled et al., 1991). Non-smooth-muscle sources are likely to provide at most a minor contribution to the number of distal arteriole SMCs, yet further experiments are indicated that utilize rigorous fate mapping (with conditional cell-specific labeling when appropriate) and analyze the distal arteriole beds delineated herein.

Although alveolar myofibroblasts are extremely rare in the normal adult, they are present in the lungs of PH patients and are implicated in disease pathophysiology (Chen et al., 2006; Choi, 2010; Kapanci et al., 1990). Previously, it was shown that mice exposed to 6 weeks of hypoxia have increased alveolar SMA^{+} cells, and their formation is enhanced by transforming growth factor β-dependent signaling (Chen et al., 2006). Herein, we find a significant increase in alveolar myofibroblasts by 7 days of hypoxia, and by 21 days, most of these SMA^{+} alveolar cells also express SMMHC, traditionally considered a specific marker of SMCs (Miano et al., 1994). Moreover, in contrast to distal pulmonary arteriole SMCs, we show that the vast majority of alveolar myofibroblasts derive from SMA^{−} cells and that proliferation of SMA[+] myofibroblasts is very rare. Thus, our findings with regard to hypoxia-induced alveolar myofibroblasts are the following: (1) early appearance of myofibroblasts, (2) SMMHC expression, (3) predominant SMA[−] cellular origin, and (4) negligible proliferation. Taken together, we show that hypoxia induces robust and early expansion of an alveolar SMA[+]SMMHC[+] myofibroblast population largely through differentiation of SMA^{−} cells.

Our approach of analyzing specific distal pulmonary arteriole beds over time during PH onset is a paradigm shift from standard analysis of random lung sections and allows for the evaluation of cellular and molecular dynamics during arteriole muscularization. In response to hypoxia, our results indicate that pre-existing differentiated SMCs dedifferentiate and then follow a very similar muscularization program to that of the developing PA (schematic Figure 4D) (Greif et al., 2012). Initially, SMMHC[+]SMA^{+} cells downregulate SMMHC and upregulate PDGFR-β expression and migrate across the M-D arteriole border (day 3). These distal arteriole undifferentiated cells then proliferate robustly and continue to migrate distally (day 7). By 14 days of hypoxia, the distal arteriole SMA^{+} cells begin to reduce PDGFR-β expression and upregulate SMMHC, and at 21 days, the distal arteriole is muscularized by differentiated, mature SMCs, similar to the normoxic middle arteriole. These newly muscularized distal arterioles form a single layer of SMCs, and thus pathological SMA[+] progenitors migrate axially along the EC tube as in development, but in contrast to large PA morphogenesis, they do not migrate radially outward (Greif et al., 2012). Similar to development (Hellström et al., 1999), we hypothesize that signals emanating from ECs (in this case from the very distal arteriole in proximity to the capillary transition) drive the directed axial SMC migration. Interestingly, we consistently detect a few SMA[+]SMMHC[+]PDGFR-β^{+} cells adjacent to the arteriole muscular-unmuscular transition in normoxia (Figures 4D and S4A). We propose that these cells are primed to dedifferentiate, migrate and proliferate in response to insults such as hypoxia and thus, may be important players in initiating pathological distal arteriole muscularization. Addition-

ally, rodents returned to normoxia after extended hypoxia exposure have been shown to undergo reverse remodeling with a reduction in PA muscularization (Meyrick and Reid, 1980; Sakao et al., 2010), and an in-depth analysis of this intriguing process will be a focus of future investigation. In sum, we suggest that the in vivo reductionist approach utilized herein should be adopted widely to the study of vascular disease because, as in this initial example of PH, it promises to identify important previously unknown pathological events that are potential targets for novel therapeutics.

EXPERIMENTAL PROCEDURES

Animals and Tamoxifen Treatment
All animal experiments were approved by the Institutional Animal Care and Use Committee at Yale University. Mouse strains are described in Supplemental Information. For fate mapping, 2- to 4-month-old mice were injected with 1 mg tamoxifen per day for 5 days and then allowed to rest for 5 days prior to hypoxia treatment.

Hypoxia Treatment and Assessment of Right Ventricular Systolic Pressure and Hypertrophy
Mice were exposed to hypoxia (FiO_2 10%) for up to 3 weeks in a rodent hypoxia chamber with a calibrated oxygen controller and sensor (BioSpherix). Right ventricular (equivalent to PA) systolic pressures were measured by inserting a catheter (Millar Instruments) into the right ventricle via the right jugular vein, and mice were then sacrificed, the heart dissected, and the weight ratio of the right ventricle/(left ventricle + septum) assessed (Hayashida et al., 2005; Kim et al., 2013).

BrdU Labeling
For the analysis of cell proliferation, mice were intraperitoneally injected with bromodeoxyuridine (BrdU; 100 mg/kg body weight). Four hours after injection, mice were sacrificed, and the lung tissue was prepared for immunohistochemistry as described below except for 30 min incubation in 2M HCl prior to sectioning.

Lung Preparation
Mice were sacrificed by isoflurane inhalation. The pulmonary vasculature was flushed with PBS by inserting a needle connected to a reservoir into the right ventricle and allowing the fluid to drain through an incision in the thoracic aorta. Animals were then tracheostomized with an angiocatheter, and the lungs inflated with 2% low-melt agarose in PBS. Agarose-filled lungs were solidified by 30 min incubation in ice-cold PBS. Lobes were separated, fixed in Dent's fixative (4:1 methanol:DMSO) at 4°C overnight, washed in 100% methanol, bleached in 5% H_2O_2 and rehydrated into PBS. Rehydrated lungs were vibratome-sectioned at a thickness of 150 μm.

Immunohistochemical Analysis
Vibratome sections were blocked with 5% normal goat serum in 0.5% Triton X-100/PBS (PBS-T) at 4°C overnight. Sections were then incubated in primary antibodies for 1–3 days at 4°C, washed 5 × 1 hr in PBS-T, incubated in secondary antibodies overnight at 4°C, washed 3 × 1 hr in PBS-T, and placed on slides in mounting media (DAKO). Antibodies are listed in Supplemental Experimental Procedures.

Imaging
Samples were imaged on confocal microscopes (Perkin Elmer UltraView VOX spinning disc or Leica SP5 point-scanning). Volocity software (Perkin Elmer) was used to process images and count cells, and Adobe Photoshop was used to process images.

Statistical Analysis
Multifactor ANOVA and post hoc test with Bonferroni corrections were used to analyze the data (StatPlus software). All data are presented as mean ± SD.

REFERENCES

Arciniegas, E., Ponce, L., Hartt, Y., Graterol, A., and Carlini, R.G. (2000). Intimal thickening involves transdifferentiation of embryonic endothelial cells. Anat. Rec. 258, 47–57.

Chen, Y.F., Feng, J.A., Li, P., Xing, D., Zhang, Y., Serra, R., Ambalavanan, N., Majid-Hassan, E., and Oparil, S. (2006). Dominant negative mutation of the TGF-beta receptor blocks hypoxia-induced pulmonary vascular remodeling. J. Appl. Physiol. 100, 564–571.

Choi, C.W. (2010). Lung interstitial cells during alveolarization. Korean J Pediatr. 53, 979–984.

Farber, H.W., and Loscalzo, J. (2004). Pulmonary arterial hypertension. N. Engl. J. Med. 351, 1655–1665.

Gomez, D., and Owens, G.K. (2012). Smooth muscle cell phenotypic switching in atherosclerosis. Cardiovasc. Res. 95, 156–164.

Greif, D.M., Kumar, M., Lighthouse, J.K., Hum, J., An, A., Ding, L., Red-Horse, K., Espinoza, F.H., Olson, L., Offermanns, S., and Krasnow, M.A. (2012). Radial construction of an arterial wall. Dev. Cell 23, 482–493.

Hayashida, K., Fujita, J., Miyake, Y., Kawada, H., Ando, K., Ogawa, S., and Fukuda, K. (2005). Bone marrow-derived cells contribute to pulmonary vascular remodeling in hypoxia-induced pulmonary hypertension. Chest 127, 1793–1798.

Hellström, M., Kalén, M., Lindahl, P., Abramsson, A., and Betsholtz, C. (1999). Role of PDGF-B and PDGFR-beta in recruitment of vascular smooth muscle cells and pericytes during embryonic blood vessel formation in the mouse. Development 126, 3047–3055.

Humbert, M., Sitbon, O., Chaouat, A., Bertocchi, M., Habib, G., Gressin, V., Yaïci, A., Weitzenblum, E., Cordier, J.F., Chabot, F., et al. (2010). Survival in patients with idiopathic, familial, and anorexigen-associated pulmonary arterial hypertension in the modern management era. Circulation 122, 156–163.

Jiao, K., Langworthy, M., Batts, L., Brown, C.B., Moses, H.L., and Baldwin, H.S. (2006). Tgfbeta signaling is required for atrioventricular cushion mesenchyme remodeling during in vivo cardiac development. Development 133, 4585–4593.

Kapanci, Y., Burgan, S., Pietra, G.G., Conne, B., and Gabbiani, G. (1990). Modulation of actin isoform expression in alveolar myofibroblasts (contractile interstitial cells) during pulmonary hypertension. Am. J. Pathol. 136, 881–889.

Kim, J., Kang, Y., Kojima, Y., Lighthouse, J.K., Hu, X., Aldred, M.A., McLean, D.L., Park, H., Comhair, S.A., Greif, D.M., et al. (2013). An endothelial apelin-FGF link mediated by miR-424 and miR-503 is disrupted in pulmonary arterial hypertension. Nat. Med. 19, 74–82.

Mahapatra, S., Nishimura, R.A., Sorajja, P., Cha, S., and McGoon, M.D. (2006). Relationship of pulmonary arterial capacitance and mortality in idiopathic pulmonary arterial hypertension. J. Am. Coll. Cardiol. 47, 799–803.

McGowan, S.E., and McCoy, D.M. (2011). Fibroblasts expressing PDGF-receptor-alpha diminish during alveolar septal thinning in mice. Pediatr. Res. 70, 44–49.

Metzger, R.J., Klein, O.D., Martin, G.R., and Krasnow, M.A. (2008). The branching programme of mouse lung development. Nature 453, 745–750.

Meyrick, B., and Reid, L. (1980). Hypoxia-induced structural changes in the media and adventitia of the rat hilar pulmonary artery and their regression. Am. J. Pathol. 100, 151–178.

Miano, J.M., Cserjesi, P., Ligon, K.L., Periasamy, M., and Olson, E.N. (1994). Smooth muscle myosin heavy chain exclusively marks the smooth muscle lineage during mouse embryogenesis. Circ. Res. 75, 803–812.

Morimoto, M., Liu, Z., Cheng, H.T., Winters, N., Bader, D., and Kopan, R. (2010). Canonical Notch signaling in the developing lung is required for determination of arterial smooth muscle cells and selection of Clara versus ciliated cell fate. J. Cell Sci. 123, 213–224.

Morrell, N.W., Adnot, S., Archer, S.L., Dupuis, J., Jones, P.L., MacLean, M.R., McMurtry, I.F., Stenmark, K.R., Thistlethwaite, P.A., Weissmann, N., et al. (2009). Cellular and molecular basis of pulmonary arterial hypertension. J. Am. Coll. Cardiol. 54 (1, Suppl), S20–S31.

Muzumdar, M.D., Tasic, B., Miyamichi, K., Li, L., and Luo, L. (2007). A global double-fluorescent Cre reporter mouse. Genesis 45, 593–605.

Peled, A., Zipori, D., Abramsky, O., Ovadia, H., and Shezen, E. (1991). Expression of alpha-smooth muscle actin in murine bone marrow stromal cells. Blood 78, 304–309.

Qiao, L., Nishimura, T., Shi, L., Sessions, D., Thrasher, A., Trudell, J.R., Berry, G.J., Pearl, R.G., and Kao, P.N. (2013). Endothelial fate-mapping in mice with pulmonary hypertension. Circulation 129, 692–703.

Rabinovitch, M. (2008). Molecular pathogenesis of pulmonary arterial hypertension. J. Clin. Invest. 118, 2372–2379.

Sakao, S., Tatsumi, K., and Voelkel, N.F. (2010). Reversible or irreversible remodeling in pulmonary arterial hypertension. Am. J. Respir. Cell Mol. Biol. 43, 629–634.

Seidelmann, S.B., Lighthouse, J.K., and Greif, D.M. (2013). Development and pathologies of the arterial wall. Cell. Mol. Life Sci. Published online September 27, 2013. http://dx.doi.org/10.1007/s00018-013-1478-y.

Shimoda, L.A., and Laurie, S.S. (2013). Vascular remodeling in pulmonary hypertension. J. Mol. Med. 91, 297–309.

Spees, J.L., Whitney, M.J., Sullivan, D.E., Lasky, J.A., Laboy, M., Ylostalo, J., and Prockop, D.J. (2008). Bone marrow progenitor cells contribute to repair and remodeling of the lung and heart in a rat model of progressive pulmonary hypertension. FASEB J. 22, 1226–1236.

Stenmark, K.R., Fagan, K.A., and Frid, M.G. (2006). Hypoxia-induced pulmonary vascular remodeling: cellular and molecular mechanisms. Circ. Res. 99, 675–691.

Wendling, O., Bornert, J.M., Chambon, P., and Metzger, D. (2009). Efficient temporally-controlled targeted mutagenesis in smooth muscle cells of the adult mouse. Genesis 47, 14–18.